Comparative analysis of topologies to integrate photovoltaic sources in the feeder stations of AC railways

D'Arco, S.; Piegari, L.; Tricoli, P.

DOI:
10.1109/TTE.2018.2867279

Comparative Analysis of Topologies to Integrate Photovoltaic Sources in the Feeder Stations of ac Railways

S. D'Arco, L. Piegari, *Senior Member, IEEE*, and P. Tricoli, *Member, IEEE*

***Abstract*— The increasing diffusion of renewable energy sources in the power systems is likely to extend in the near future to power supply of railways. This paper compares the technical and economic benefits of several configurations with power electronics converters for the integration of photovoltaic sources into the railway power supply systems. For each of these configurations, a design methodology is proposed for selecting the ratings of the railway power supply components. The requirements for the phase imbalance on the feeding transmission line are assumed in accordance with current regulatory standards and, wherever necessary, phase balancers are added. The design methodology is applied to the power supply of a high-speed railway and the configurations under study are numerically compared based on their technical feasibility and economic cost, using the generation capacity of the photovoltaic source as independent variable. The analysis demonstrates that with a progressive integration of PV sources into railway systems, the configurations with power converters supplying the overhead lines could become more beneficial than more classical solutions where the overhead line is supplied via a transformer.**

***Index Terms*— ac-ac converters, photovoltaic cells, railway engineering, traction power supplies.**

I. Introduction

The integration of renewable energy sources into railway power systems has been so far relatively limited. However, due to technological improvements and to the drastic reduction of installation and operating costs, renewable energy sources are expected to play a much more important role in future railway electrification systems. Present trends indicate a steady increase of the energy consumption of railways, primarily due to growing traffic conditions and faster trains. This often leads to the necessity of upgrading the railway power supply by adding new connections to the high-voltage public grid, with consequent technical challenges and high costs. The installation of renewable energy sources in the proximity of railway feeder stations could mitigate the impact on the public grid of the higher power demand from the railway. Photovoltaic (PV) panels are inherently suitable for railways integration, since large spaces are normally available at the rooftop of stations, trackside land and surrounding parking lots [1], [2]. Examples of existing installations are a 390 kW roof-top photovoltaic system at Tokyo station in 2011, a 78 kW photovoltaic system with 240 kWh lithium-ion batteries at Hiraizumi station in 2012 both by East Japan Railways [3], and a 522.12 kW of solar power generation capacity in Korea, including a 90.4 kW rooftop photovoltaic system at Korail headquarters building[4]. The initial field trials proved that there is a strong potential for future usage of PV as technology is continuously improving and their cost is steadily decreasing. PV sources, with the support of energy storage, could be also controlled to provide auxiliary services to the grid, such as reactive power and harmonic compensation [5], or to end-users, such as battery recharging of electric vehicles [6]. With specific reference to railways, it has been shown that a suitable control of PV sources and energy storage can save energy and reduces running costs [7], [8], [9]. PV sources and energy storage operates typically at low voltage dc and, hence, require power converters for the connection to the railway electrification system, which instead is fed at either 25 kV ac at 50 Hz, 15 kV ac at 16.67 Hz or 3 kV dc. Several connection schemes are technically feasible and it is not obvious to determine the most effective and economical configuration. The technical literature offers a few examples of detailed studies of single configurations but lacks a comparative analysis highlighting their relative advantages and drawbacks. In the following, focus will be made on ac railways only, as they are currently the most consolidated technology for the electrification of mainline and high-speed railways [10], [11], while medium voltage dc systems seem still far away from a practical implementation [12]

In general, the design choices for the power supply configurations should be aimed at improving the following disadvantages and limitations of ac railways [13], [14]:

1) high voltage drops due to the requirement of single-end feeding; single-end feeding is necessary to avoid that the overhead line constitutes a parallel path for the public grid;
2) static imbalance, being trains single-phase loads connected to a three-phase grid;

The first disadvantage can be mitigated by special traction schemes using either booster transformers or auto-transformers

S. D'Arco is with SINTEF Energy research, Trondheim, Norway (salvatore.darco@sintef.no)

L. Piegari is with the Department of Electronics, Information and Bioengineering of the Politecnico di Milano, Milan, Italy (luigi.piegari@fpolimi.it)

P. Tricoli is with the Department of Electronic, Electrical and Systems Engineering, University of Birmingham, Birmingham, UK (p.tricoli@bham.ac.uk)

This work was supported by the European Union's Horizon 2020 Research and Innovation Programme under Grant 774392.

that enable feeding sections of length up to 20-30 km. However, the sectioned overhead line strongly reduces the chances of using the braking energy inside the railway. The second disadvantage is normally addressed by either a special design of traction transformers, like Scott of Leblanc types, or a special connection, i.e. each feeding section is connected to a different pair of phases of the public grid. Both methods achieve adequate balancing only if the power absorbed by trains is the same for all the feeding sections [15]. As in practice a residual static imbalance of around 1% is always present, ac railways needs to be connected to high-voltage grids, typically at 132 kV or 400 kV, to minimise any distortion of the voltage caused by the imbalance. The obvious drawback of this choice is the high cost of connection and the difficulty in locating suitable connection points. When the level of balancing required by the grid operator is stricter, an additional phase balancer is needed [16]. This solution has been adopted for high-speed lines in Japan [17] and in China [18] and mainly consists of a static converter that dynamically injects a negative sequence current to compensate for the single-phase power drawn by the trains. Due to the increasing diffusion of renewable sources and reduction of power system's inertia, it is expected that future electric railways will not be allowed to introduce any imbalance on the grid and, hence, in this analysis the presence of a phase balancer will be considered strictly necessary.

The easiest and most obvious solution for integrating PV sources is to connect them to the high-voltage busbars of the transformers of railway feeder stations with no modifications on the railway side. This configuration is assumed in this paper as the baseline for the comparison of other four power configurations with power converters to exploit the potential of PV sources while addressing the shortcomings of ac railways. The five configurations are first described with brief considerations on their rationale. Moreover, a methodology is established for determining the ratings of the main components as power converters and transformers.

The methodology is then applied to a sample case of a high-speed railway and a technical and economic analysis is numerically carried out to evaluate the capital cost of the components and the electricity cost due to power losses [19]. Finally, based on the results of the numerical analysis, the paper highlights the relative merits of each configuration and provides recommendations for the design of railway power supplies with integrated PV generation.

II. Power Configurations for the Integration of PV Sources in Railway Systems

This section introduces the five configurations with power electronics converters for the integration of PV into the railway electrification system. These configurations, shown in Fig. 1, are selected to be functionally equivalent and present the following common characteristics:

- a 25 kV, 50 Hz single-phase ac railway overhead line supplied by feeder stations connected to a high-voltage public grid at 132 kV;
- the railway is not allowed to introduce phase imbalance on the transmission grid; this is guaranteed either by three-phase power converters in the feeder stations or by extra phase balancers;
- a PV source is located in the proximity of each railway feeder station.

Fig. 1a shows the baseline configuration *"a"*, which assumes that the single-phase transformer, the PV source, and the phase balancer are all connected in parallel to the high-voltage bus bars [20]. The phase balancer is rated for few kV and consists of a three-phase converter and a three-phase transformer in accordance with the limits of semiconductor devices currently available on the market [21] and the typical 3-level converter topology for high-power applications [22],[23]. In general, one phase balancer could suffice for three adjacent feeder stations and, thus, a phase balancer with one third of the power rating is assumed in each feeder station. The PV generator operates at lower voltage (around 1 kV) and is connected to the grid with a three-phase inverter and transformer.

The configuration *"b"* (in Fig. 1b) proposed by the authors, is derived from the configuration *a* by merging together the converters and the transformers of the phase balancer and the PV source. Thus, the PV generator is connected to the dc circuit of the phase balancer with a dc-dc boost converter to adapt the voltage and enable the maximum power point tracking control.

In the third configuration, *"c"*, also proposed by the authors (Fig. 1c), the PV generator is connected to the overhead line via a single-phase inverter operating at low voltage and a single-phase transformer to step up the voltage to 25 kV. The phase balancer is independently connected to the grid via a three-phase transformer as in Fig. 1a.

In the remaining two configurations, the railway power supply, the PV generator, and the phase balancer are merged together with a multiple-input static converter [24]. The most important difference from the previous configurations is that the sectioning of the railway overhead line is no longer needed and the railway can be supplied simultaneously from several feeder stations. In the configuration *"d"* (Fig. 1d) the ac-dc input stage of the converter is a bidirectional three-phase active rectifier, while in the configuration *"e"* (Fig. 1e) it is a unidirectional diode rectifier. As a direct implication of the diode rectifier in the fifth configuration, there is no need of a special control to avoid recirculation of power between the three-phase grid and the railway. However, this scheme requires an extra energy buffer to absorb the excess energy generated by the PV and train braking if there is insufficient demand on the railway line. Thus, the configuration includes an additional storage unit connected to the dc-bus via a second bi-directional boost dc-dc converter. The energy storage could be added also to the configuration *d*, which would also be equivalent of replacing the diode rectifier with a bi-directional converter as in configuration *e*. However, this additional topology would increase the cost with only a marginal benefit for the entire system, as the electricity surplus from the PV could be directly transferred to the grid, making the energy storage redundant. For this reason, this configuration has not been included in this paper.

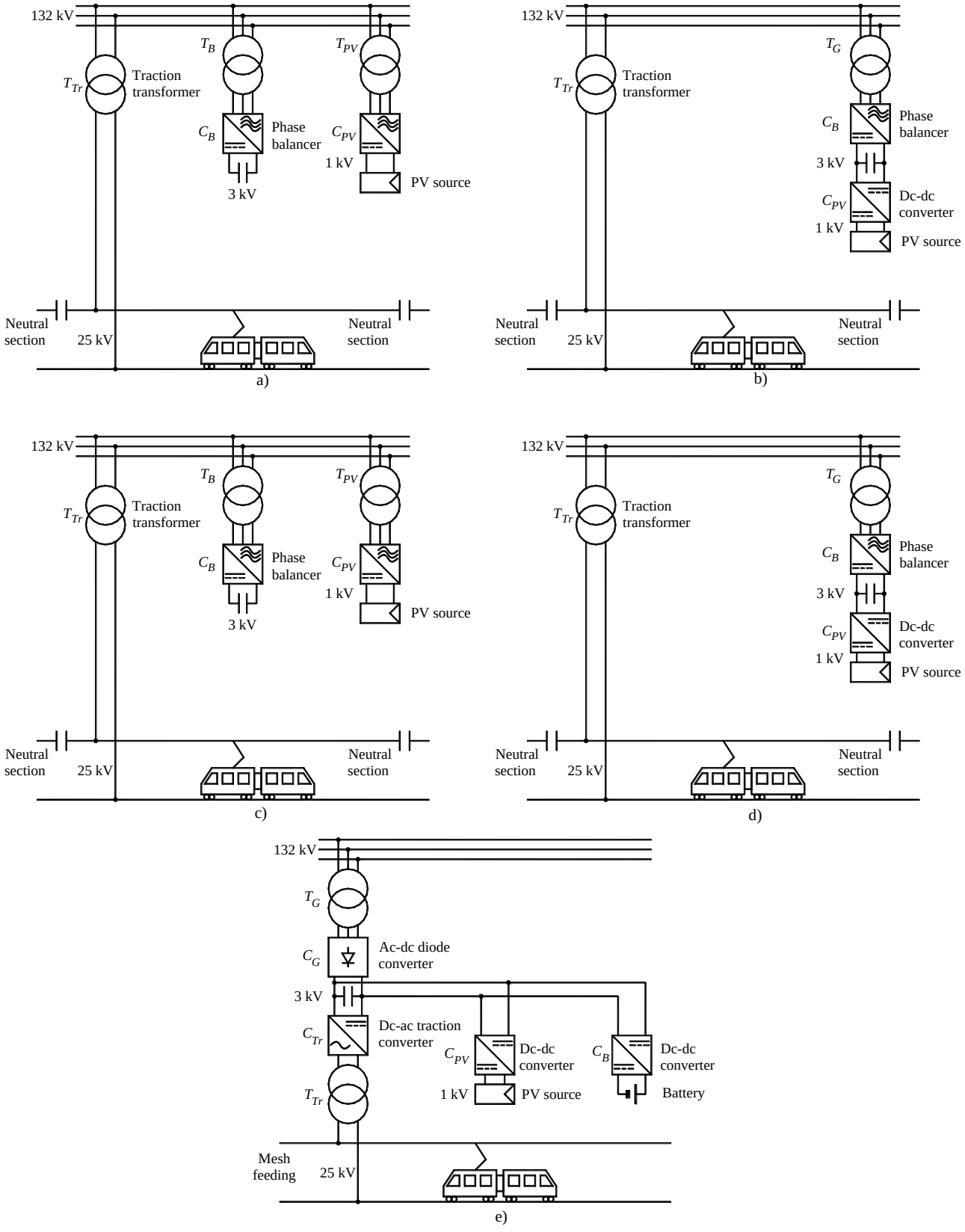

Fig. 1. Connection schemes for integration of PV to railway feeder stations considered in this study

III. Efficiency Analysis and Preliminary Design of the Proposed Configurations

This section presents the fundamental steps of the design methodology for determining the ratings of the components for the five configurations previously described. The design is reported separately for each configuration in a dedicated

subsection, except for the parts common to all configurations that are presented together at the beginning. For a fair cost comparison, the different configurations are designed to offer equivalent performance for the railway and the grid. Moreover, power losses are assumed to have a negligible effect on the power ratings and, hence, they are taken into account only for calculating operating costs.

In the following, it is assumed that the instantaneous train power, $P_{tr}(t)$, and the instantaneous power generated by the PV, $P_{pv}(t)$, are given as inputs for the design. The rated power $P_{Cx,n}$ of a converter C_x, is determined on the basis on the maximum instantaneous power, as converters have a limited overloading capability. Transformers allow instead temporary overloading, with a typical thermal time constant of about 60 minutes and a peak power of about 300% of the nominal power for a few seconds. Therefore, the rated power $P_{Tx,n}$ of a transformer T_x, has been calculated as the maximum between the highest average power over any time interval of 60 minutes and a third of the peak power. This leads to:

$$P_{Cx,n} = \max\left[\left|P_{Cx}(t)\right|\right]$$
$$P_{Tx,n} = \max\left[\int_{60\,\min}\left|P_{Tx}(t)\right|dt, \frac{\max\left(\left|P_{Tx}(t)\right|\right)}{3}\right] \quad (1)$$

where $P_{Cx}(t)$ and $P_{Tx}(t)$ are the instantaneous powers of converter C_x and transformer T_x, respectively.

As Fig. 1 shows, all the configurations include a single-phase traction transformer for the overhead line, T_{tr}. Additionally, for all the configurations but configuration *c*, the power to the railway is fed entirely by T_{tr} and, hence:

$$P_{T_{tr}}(t) = P_{tr}(t). \quad (2)$$

Similarly, the instantaneous power generated by the PV is equal to the power of the converter P_{CPV} interfacing the PV panels and, therefore:

$$P_{C_{pv}}(t) = P_{PV}(t). \quad (3)$$

Moreover, it is assumed that the conversion efficiency is independent on the power rating and that the power losses are the sum of a constant term and a term proportional to the power squared. This is because power losses are proportional to the square of the current and the voltage is approximately constant and, thus, power and current are proportional. Therefore, for the power losses of each component of the system, either a transformer or a converter, the following simplified model is assumed [25]:

$$P_{loss.x} = \left\{k_{0,x} + k_{1,x}\left[\frac{P_x(t)}{P_{x,n}}\right]^2\right\}P_{x,n}. \quad (4)$$

where $k_{0,x}$ and $k_{1,x}$ are constants depending on the specific converter or transformer. Equation (4) shows that power losses increase quadratically with the per-unit power and are assumed proportional to the power rating of converters or transformers for the same per-unit power.

The cost of each electrical component is modelled for both transformers and converters as the sum of a fixed cost and a cost linearly increasing with the power rating:

$$C_x = c_{0,x} + c_{1,x}P_{x,n}, \quad (5)$$

where $c_{0,x}$ and $c_{1,x}$ are constants depending on the specific converter or transformer.

A. Design of configuration a

With reference to configuration *a*, the entire photovoltaic power flows through the transformer T_{pv}, and therefore the two powers are equal when neglecting the power losses:

$$P_{T_{pv}}(t) = P_{pv}(t). \quad (6)$$

In this configuration the overhead line is connected to the grid via a single-phase transformer and the adjacent sections are connected to different phases of the grid, so that the system is balanced every three feeder stations. Thus, if the load is equal for three consecutive feeder stations, the grid would not be affected by any imbalance. In practice this condition does not happen and a phase balancer is required. In the worst-case scenario, only one feeder station is loaded with a power P_{tr}, leading to the maximum imbalance to be compensated for. For this condition, the rated power of each phase balancer is equal to $P_{tr}/3$, as it has been assumed one phase balancer per feeder station. Assuming identical phase balancers for each feeder station the power of the converter of the phase balancer is:

$$P_{C_b}(t) = P_{Tb}(t) = \frac{P_{tr}(t)}{3} \quad (7)$$

as the power of the phase balancer flows entirely through the converter C_b and the transformer T_b.

B. Design of configuration b

For this configuration, the converter C_b operates both as a phase balancer and as the interface for the PV source. The entire power flows through the three-phase transformer connecting the converter C_b to the grid. Thus, the powers of the converter C_b and the transformer T_g are given by:

$$P_{T_g}(t) = P_{C_b}(t) = \max\left[P_{pv}(t), \frac{P_{tr}(t)}{3}\right] \quad (8)$$

C. Design of configuration c

For this configuration, the transformer T_{pv} is directly connected to the PV source and, hence:

$$P_{T_{pv}}(t) = P_{pv}(t). \quad (9)$$

The difference between the train power and the PV generation flows across the transformer T_{tr}:

$$P_{T_{tr}}(t) = P_{tr}(t) - P_{pv}(t). \quad (10)$$

The power of the converter of the phase balancer can be calculated as it has been done for configuration *a*. Indeed, the two configurations are conceptually identical, except that the power of C_b and T_b are respectively:

$$P_{C_b}(t) = P_{T_b}(t) = \frac{1}{3}\left[P_{tr}(t) - P_{pv}(t)\right]. \quad (11)$$

As in (11) the PV generation is variable during the day and the system must operate also when there is no sun, it is assumed $P_{pv} = 0$ for the design of C_b and T_b.

D. Design of configuration d

For this configuration, the entire train load flows through the single-phase converter C_{tr} and, thus:

$$P_{C_{tr}}(t) = P_{tr}(t). \quad (12)$$

The three-phase converter C_g processes the power exchanged with the grid, which is equal to the difference between the power of the train load and the power generated by the PV unit:

$$P_{C_g}(t) = P_{tr}(t) - P_{pv}(t). \quad (13)$$

Due to variability of the photovoltaic generation, the converter C_g and the transformer T_g transmit either the entire traction power P_{tr} in case of no PV generation, or the entire PV power P_{pv} in case of no traction load, or the difference between the two powers for all the other cases. Therefore, the power ratings of C_g and T_g are calculated as follows:

$$P_{C_g}(t) = P_{T_g}(t) = \max\left[\left|P_{tr}(t)\right|, \left|P_{pv}(t)\right|, \left|P_{tr}(t) - P_{pv}(t)\right|\right]. \quad (14)$$

E. Design of configuration e

For this configuration, the converter C_g is a diode rectifier and the power flows from the grid to the railway only. As the power of this converter is always positive and equal to the difference between the traction load and the sum of the PV generation and the battery power, it is possible to write the following equation:

$$P_{C_g} = \max\left[P_{tr}(t), P_{tr}(t) - P_{pv}(t) - P_b(t), 0\right]. \quad (15)$$

As in the previous case, the power of converter C_g is chosen without considering the contributions of the PV and the battery to ensure that the system is working also with no sun and an empty battery, so the design equation is:

$$P_{C_g} = \max\left[P_{tr}(t), 0\right]. \quad (16)$$

In order to design the converter of the battery C_b, it is necessary first to decide a control strategy for the battery itself. The main goal of the battery is to store all the PV energy surplus not used by the trains. For this reason, to minimise the storage capacity, the battery is charged only when the PV power is higher than the train power. Otherwise, the battery is discharged up to its rated current. For this reason, the converter of the battery is designed according to the following equation:

$$P_{C_b}(t) = \max\left(\left[P_{pv}(t) - P_{tr}(t)\right], 0\right). \quad (17)$$

There could be situations where the PV could generate a surplus that cannot be stored in the battery or used by the trains. It should be noted that this does not represent an issue as the MPPT control of the PV converter would stop generation by sensing the increase of the common dc bus voltage. Also, the railway electrification system is not affected by faults of the battery and/or the PV source, as the power to the trains can be entirely supplied by the converters C_g and C_{tr}.

IV. Case Study

The configurations presented in section II have been compared for a sample case study of a high-speed railway fed at 2x25 kV, 50 Hz considering only the cost of the electrical components. This is because the costs of project management and civil construction, which represent a significant share of the total cost of a feeder station, are uniquely related to the specific location and, hence, almost independent on the particular choice of the electrical configuration. Moreover, there is a limited number of existing locations where PV sources have been directly integrated with railway systems and mainly for research trials. Their costs are not representative of commercial products and, hence, are not considered in this paper.

The different arrangement of the railway electrification system of the five configuration has an implication on the distance between the feeder stations. In configurations *a*, *b* and *c*, the line is directly fed by a single-phase transformer and the feeding sections are electrically isolated to avoid phase-to-phase short circuits. Thus, the distance between two consecutive feeding stations is calculated from the maximum voltage drop allowed on the line which is given by the line impedance and the train power. By contrast, in configurations *d* and *e* the line is fed simultaneously from all the feeder stations. This effectively reduces by half the number of feeder stations required when the maximum voltage drop on the line is the same, which has been taken into account in the calculation of costs.

The case study assumes the presence of a PV generation at each feeder station with simplified profiles for the power demand of the trains. More specifically, the same PV power has been assumed for all the feeder station using the annual sun irradiation of an Italian site [26] scaled on the basis of the maximum installed PV power. Three scenarios have been evaluated for each configuration:1 MW, 7.5 MW and 15 MW of installed PV power for *a*, *b*, and *c* and 2 MW, 15 MW and 30 MW for the *d* and *e* to take into account the different number of feeder stations.

The diagram of the load power demand for each feeder station is shown in Fig. 2a for configurations *a*, *b* and *c*, and in Fig. 2b for configurations *d* and *e*. The power demand assumes trains travelling between 8:00 and 21:00 with a headway of 10 minutes during peak hours (8:00-10:00 and 15:00-18:00) and of 15 minutes otherwise. Trains travelling in opposite directions are assumed with the same daily frequency but with a departing time delayed by 3 minutes. The power drawn by the trains depends on their speed and acceleration but usually high speed trains travel at maximum cruising speed and draw a constant power equal to the rated one [27]. Taking into account that the focus of this paper is to design the feeder station components and that the railway must correctly operate in the worst-case scenario, each train is modelled as a constant 10 MW load travelling on the line at a maximum speed of 300 km/h. This means that the distance between the trains is 50 km at peak time and 75 km at off-peak time. The maximum distance between two feeder stations is based on a minimum line voltage of 19 kV, as indicated by EU standard EN 50163 and the line impedance is assumed equal to 516 mΩ/km. That means that the distance between the feeder stations is approximately 22 km for configurations *a*, *b* and *c*, and approximately 44 km for configurations *d* and *e*. For the assumed scheduled timetable, there is a maximum of 2 trains simultaneously present in the same section for all the configurations.

Figure 2 shows the daily power diagram supplied by a feeder

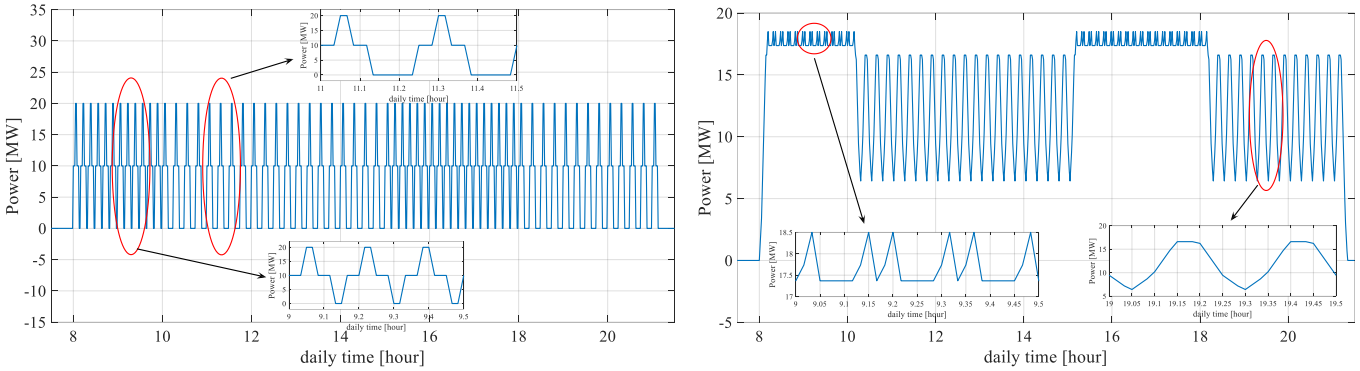

Fig. 2. Diagrams of the daily power of each feeder station: a) configurations *a*, *b* and *c*; b) configurations *d* and *e*.

station with a data point every minute. In particular, Fig. 2a refers to configurations *a*, *b* and *c* while Fig. 2b refers to configurations *d* and *e*. For configurations *a*, *b* and *c* each feeder station feeds entirely the trains located within its feeding section. For the assumed scheduled timetable, a maximum of two trains are simultaneously present in the same feeding section and the diagram of the power changes with steps of 10 MW, i.e. 0 MW when there are no trains, 10 MW when there is one train and 20 MW when there are two trains. Hence, the maximum power of a feeder station is 20 MW. For configurations *d* and *e*, each section is supplied by two feeder stations. The power for each train (10 MW) is supplied by the nearest two feeder stations inversely proportional to their distance from the train. Therefore, the power of a feeder station increases when the train is travelling towards it, reaches the maximum when the train is at the feeder station and decreases when the train moves away from it.

In configuration *e*, the rated power of the battery is the difference between the traction and the PV powers. Since the battery control system aims at storing all the surplus energy generated by the PV, the excess energy is stored in the battery when the generated power is higher than the power drawn by the railway. When the train power is instead higher than the generated power, the battery is discharged up to its nominal power. The total energy of the battery can be calculated by simulating the operations of the railway over one working day, assuming a maximum depth of discharge of the battery equal 80% to ensure the expected lifetime. The data used for the numerical simulations are reported in Table I.

TABLE I. MAIN DATA USED FOR THE SIMULATIONS

	k_0 [p.u.]	k_1 [p.u.]	c_0 [k€]	c_1 [k€/MW]
Single-phase transformer	0.0015	0.003	5	12.5
Three-phase transformer	0.0015	0.003	5	10
Single-phase dc/ac converter	0.005	0.015	25	100
Three-phase dc/ac converter	0.005	0.015	25	67
dc/dc converter	0.005	0.015	25	33
Diode bridge rectifier	0.005	0.015	0	1

The specific cost of the battery has been chosen equal to 150 k€/MWh, while the price of electrical energy has been set at 0.1 k€/MWh. In the numerical analysis, the installation costs and the costs associated to energy losses per km of line for the five configurations are displayed in Fig. 3. It is worth noting that when the total line length increases, the cost functions present a discontinuity when an extra feeder station is necessary to keep the maximum voltage drop within the given limit. The effect of the discontinuity is smoothed out for longer lines, because the total cost of the electrification increases with the line length, while the cost of one extra station remains the same. For a PV source of 2 MW, the railway power demand is always higher than the PV power. In particular, the power losses of configurations *d* and *e* are equal, since the same power is supplied by the same number of converters and the efficiency coefficients in (5) are all equal (corresponding to 98% efficiency at rated power).

With reference to capital cost, configuration *d* is significantly more expensive than the others because of the high cost of the bidirectional ac/dc converter C_G that has to supply the entire traction power. When instead the power of PV is substantial (15 or 30 MW), the cost of the PV converter increases for all the configurations and, hence, the cost of C_G for configuration *d* is comparable with the others. The capital cost of configuration *e* is significantly higher than the others for the large capacity of the battery.

With reference to the energy costs, configurations *d* and *e* are the most expensive, because of the power losses of converters C_G and C_{tr}, which are less efficient than transformers. The two costs are nearly the same when PV are 2 MW, because the train power is always higher than the PV power and the energy stored by the battery is very small. For higher PV powers, the power losses of these configurations do not increase significantly, as the PV source is integrated in the railway power supply and there is no need for phase balancers. For the other configurations, instead, the powers of the PV converters and the phase balancers increase and so do the power losses. As a subsequent step for the comparison, the length of the line has been set to 400 km and the total costs of the five configurations have been analysed over the years of operation, adding up together the installation and energy losses costs of Fig. 3. Assuming a life time of 20 years for the main components of the electrification system, the results are reported in Fig. 4. It can be noticed that the configuration with minimum cost depends on the rating of the PV source. For this reason, the total costs have been analysed as a function of the installed PV power and the results are shown in Fig. 5.

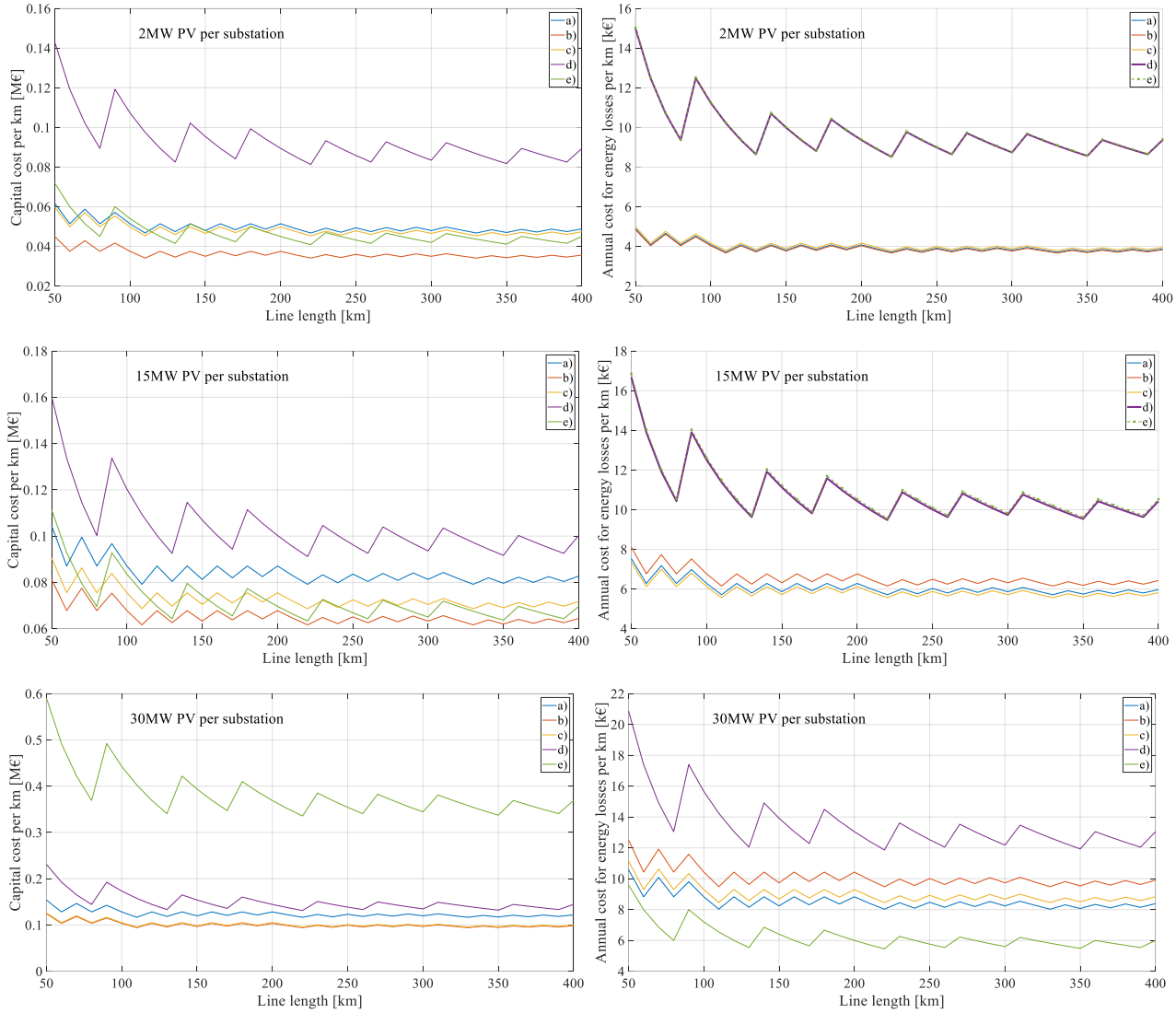

Fig. 3. Capital cost and annual energy losses cost per line km and for different installed PV powers

Among *a*, *b*, and *c*, configuration *c* is preferable for a small PV power, since the power is injected directly into the single-phase grid. As a consequence, the power to be compensated for by the phase balancer is limited and the PV power converter cost is lower, being a single-phase converter. When the size of the PV is higher than the traction power, the phase balancer compensates also the power injected into the grid and, hence, configuration *c* becomes less convenient than the other two. In the comparison between *a* and *b* for low PV power, *b* is preferable because the PV power can be injected using the phase balancer converter reducing the total cost. For high PV power, the cost of the phase balancer converter increases and *b* becomes more expensive than *a*. For configurations *d* and *e*, it is possible to conclude that configuration *e* is less expensive until the power generated by the PV is lower than the power of the trains, since it uses a diode converter. However, when the PV power increases, the cost of the energy storage becomes dominant and, hence, configuration *d* is more economical because it can directly transfer the excess power to the grid.

The five configurations present also different costs and different number of substations for the same railway and PV power. In particular, schemes *a*, *b* and *c* have a number of substations that is double than that of schemes *d* and *e*. To take into account this difference, we have defined a cost per *equivalent substation* considering only half of the substations for schemes *d* and *e*. Fig. 6 shows the variation of this cost as a function of the installed PV power and it results that, if the installed PV power is lower than the power of each feeder station (i.e. around 20 MW), configuration *e* has the lowest cost. Otherwise, due to the need of a larger battery, the cost of configuration *e* increases significantly, as confirmed by Fig. 7. For high PV power, configuration *d* has the lowest cost, suggesting the economic convenience of replacing single-phase transformers with power converters.

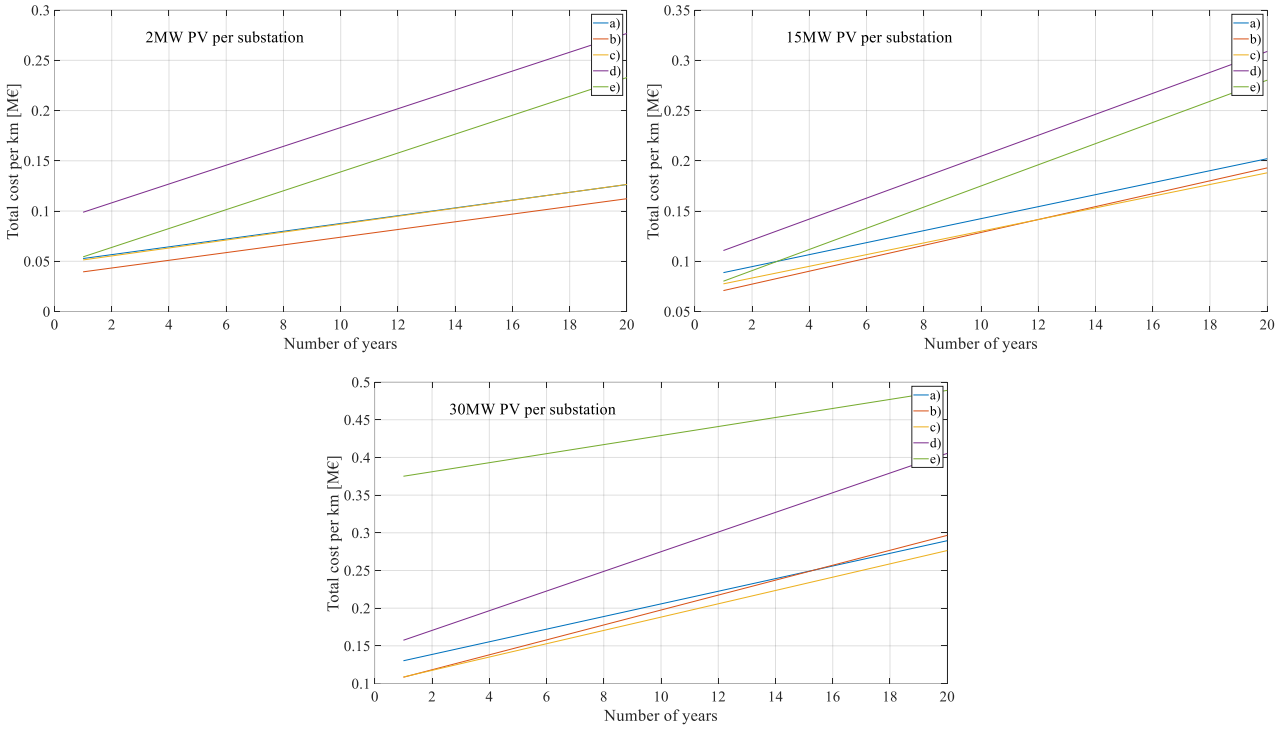

Fig. 4. Total cost as sum of the components and energy losses costs versus years of operation for different values of installed PV power

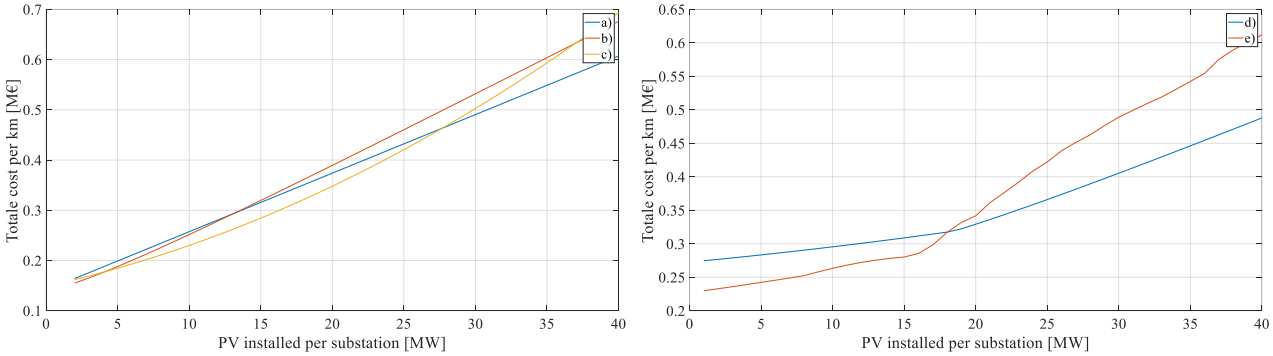

Fig. 5. Total cost of the electrification system after 20 years as a function of the installed PV power

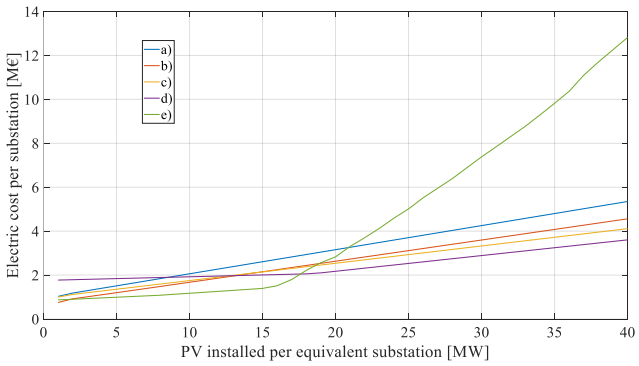

Fig. 6. Comparison of the proposed configurations in term of costs per equivalent feeder station

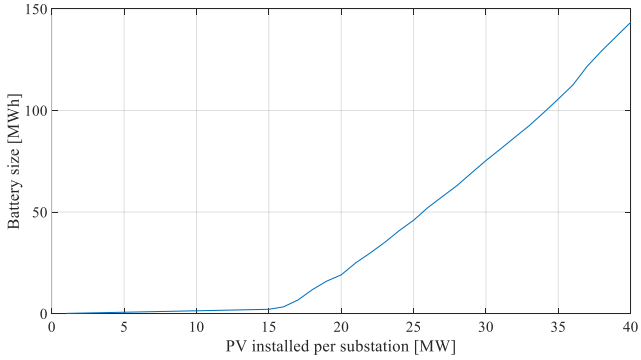

Fig. 7. Battery size versus PV power installed per feeder station

In order to better understand why the capacity of the battery increases significantly when the PV power is above 15 MW, the diagrams of the traction load, the PV power and the battery energy are reported in Fig. 8 for two values of installed PV powers of 15 MW and 25 MW, respectively. In particular, Fig. 8a refers refer to three summer days, i.e. 8th, 9th and 10th of June, while Fig. 8b refers to three winter days, i.e. 18th, 19th and 20th of December. Fig. 8a shows that, for the case of 15 MW of installed PV power, the PV power is always lower than the traction load and, due to the very limited surplus of energy

generated, the size and the cost of the battery is very small. Instead, for the case of 25 MW of installed PV power, the PV power is often higher than the traction load, so the battery has to store a large surplus of energy generated by the PV that is not consumed by the load. Fig. 8b shows that, during winter, the PV power is always lower than the railway power and the battery is not used at all.

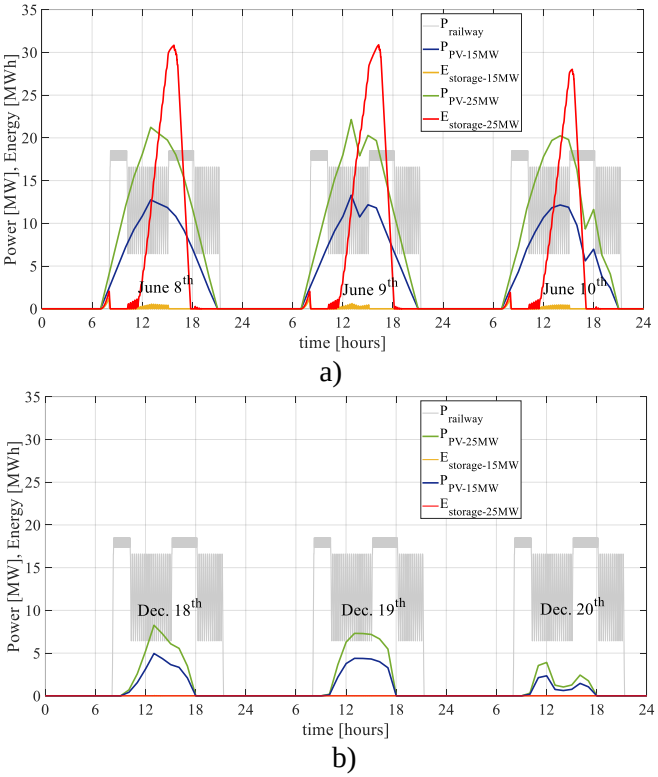

Figure 8. Railway and PV instantaneous power and energy stored for 15 MW and 25 MW installed PV power for three summer days (a) and three winter days (b).

V. Conclusion

A methodology for the design of the electrification systems of ac railways with integrated photovoltaic sources has been presented in this paper. The design considers how power converters can be arranged to minimise capital costs and power losses of the railway taking into account its typical operations. It has been shown that the power of the PV sources is a determinant factor in the choice of the most economic configuration, due to the discontinuous and variable power consumption of the railway. Numerical results on a sample railway support this hypothesis and the test case shows the details of the design criteria and their main constraints. The simulation shows that it is essential to understand whether the photovoltaic source is mainly supporting the railway or the public grid. In the first case, it is recommended using the energy storage to level out the power diagram of the railway, so a reduced amount of single-phase power has to be compensated for by the phase balancer. In the second case, it is recommended keeping the photovoltaic generation separate from the railway and using the phase balancer to minimise the imbalance caused by the railway.

The configurations with power converters used for railway traction are generally more expensive than those with transformers unless a significant photovoltaic generation is installed. Therefore, it is expected that they will become the configuration of choice when in the future a higher proportion of renewable power sources will be used to supply the electrified lines of the railways.

VI. References

[1] E. Pilo de la Fuente, S. K. Mazumder, and I. Gonzalez-Franco, “Railway electrical smart grids: an introduction to next-generation railway power systems and their operation”, *IEEE Electr. Mag.*, vol. 2, no. 3, pp. 49-55, Sep. 2014

[2] X. J. Shen, Y. Zhang, S. Chen, Y. C. Zhang, and Y.T. Yao, “Application options for grid-connected photovoltaic generation system in URT power system”, in *Proc. IET Conf. Renewable Power Gen. RPG 2011*, pp. 1-4, Edinburgh, UK, 6-8 Sept. 2011.

[3] H. Hayashiya, T. Suzuki, K. Kawahara, and T. Yamanoi, “Comparative study of investment and efficiency to reduce energy consumption in traction power supply: a present situation of regenerative energy utilization by energy storage system”, in Proc. *16th Int. Power Electron. and Motion Control Conf. and Expo. PEMC 2014*”, pp. 685-690, Antalya, Turkey, 21-24 Sept. 2014.

[4] B. J. Yoo, C. B. Park and J. Lee, “A study on design of photovoltaic system using electrical railway stations”, in *Proc. 19th Int. Conf. Electr. Machines and Sys. ICEMS 2016*, Chiba, Japan, pp. 1-5, 2016.

[5] L. Piegari and P. Tricoli, “A control algorithm of power converters in smart-grids for providing uninterruptible ancillary services”, in *Proc. 14th IEEE Int. Conf. Harmonics and Quality of Power ICHQP’10*, Bergamo, Italy, 26 29 Sep. 2010

[6] J. C. Hernandez and F. S. Sutil, “Electric vehicle charging stations fed by renewable: PV and train regenerative braking," *IEEE Latin America Trans.*, vol. 14, no. 7, pp. 3262-3269, July 2016.

[7] J. Aguado, A. J. Sanchez-Racero, and S. de la Torre, “Optimal operation of electric railways with renewable energy and electric storage systems”, *IEEE Trans. Smart Grid*, in press.

[8] P. Pankovits; J. Pouget; B. Robyns; F. Delhaye; S. Brisset, “Towards railway-smartgrid: energy management optimization for hybrid railway power substations”, in Proc. IEEE PES Innovative Smart Grid Technologies, Europe, pp. 1-6, 2014.

[9] L. Singh, C. Vaishnav, and V. Shrivastava, “Performance Analysis of Hybrid Network of Indian Traction Power System Using Renewable Energy Sources”, in Proc. 2016 Int. Conf. Micro-Electronics and Telecom. Eng. ICMETE, pp. 611-615, 2016

[10] R. D. White, “ac 25kV 50 Hz electrification supply design,” in *Proc. 6th IET Professional Development Course on Railway Electrification Infrastructure and Systems REIS 2013*, pp. 108-150, 2013.

[11] S. Hillmansen, “Electric railway traction systems and techniques for energy saving,” in *Proc. 13th IET Professional Development Course on Electric Traction Systems*, pp.1-6, 2012.

[12] A. Gómez-Expósito, J. M. Mauricio, and J. M. Maza-Ortega, “VSC-Based MVDC Railway Electrification System”, IEEE Trans. Power Del., vol. 29, no. 1, pp. 422-431, Feb. 2014.

[13] T. A. Kneschke, “Control of utility system unbalance caused by single-phase electric traction”, *IEEE Trans. Ind. Appl.*, vol. IA-21, pp. 1559–1569, Nov./Dec. 1985.

[14] I. Perin, P. F. Nussey, U. M. Cella, T. V. Tran, and G. R. Walker, “Application of power electronics in improving power quality and supply efficiency of ac traction networks”, in *Proc. IEEE 11th Int. Conf. Power Electron. and Drive Sys.*, pp. 1086-1094, 2015.

[15] T. Kneschke, “Control of Utility System Unbalance Caused by Single-Phase Electric Traction”, *IEEE Trans. Ind. Appl.* vol.IA-21, no. 6, pp.1559-1570, Nov. 1985.

[16] S. Senini and P. J. Wolfs, "Hybrid active filter for harmonically unbalanced three phase three wire railway traction loads", *IEEE Trans. Power Electron.*, vol. 15, no. 4, pp. 702-710, Jul. 2000.
[17] T. Uzuka and H. Nagasawa, "ac power supply for railways in Japan", *Elektrische Bahnen*, issue 4-5, pp. 199-206, Apr./May 2009.
[18] N.Y. Dai, K.W. Lao, M.C. Wong, and C.K. Wong, "Hybrid power quality conditioner for co-phase power supply system in electrified railway", *IET Power Electron.*, vol. 5, issue 7, pp. 1084-1094, 2012.
[19] P. J. Balducci, L. A. Schienbein, T. B. Nguyen, D. R. Brown, and E. M. Fathelrahman, "An examination of the costs and critical characteristics of electric utility distribution system capacity enhancement projects", in *Proc. 2005/2006 IEEE/PES Transm. and Distrib. Conf. and Exhibition*, pp. 78-86, 2006.
[20] J. A. Aguado, A. J. Sánchez Racero, and S. de la Torre, "Optimal operation of electric railways with renewable energy and electric storage systems, *IEEE Trans. Smart Grid*, vol. 9, no. 2, pp. 993-1001, Mar. 2018.
[21] A. Benslimane, J. Bouchnaif, M. Azizi, and K. Grari, "Study of a STATCOM used for unbalanced current compensation caused by a high-speed railway (HSR) sub-station", in *Proc. 2013 Int. Renewable and Sustainable Energy Conf.*, pp. 441-446, 2013
[22] R. Grunbaum, J.-P. Hasler, T. Larsson, and M. Meslay, "Statcom to enhance power quality and security of rail traction supply," in Proc. Advanced Electromechanical Motion Systems Electric Drives Joint Sym. ELECTROMOTION 2009, pp. 1–6.
[23] Shutian Zhang, Lin Wu, Congwei Liu, Longcheng Tan, and Qiongxuan Ge, Three-level NPC back-to-back converter with IGCT for high power ac drive", Proc. 2011 Int. Conf. on Electr. Machines and Sys., Pages: 1 – 4, 2011.
[24] A. Awasthi, A. Sinha, A. K. Singh, and R. Veeraganesan, "Solar PV fed grid integration with energy storage system for electric traction application", in Proc. 10th Int. Conf. Intelligent Sys. and Control, pp. 1-5, 2016
[25] Nema premium efficiency transformer program guidelines, https://www.nema.org, accessed on April 2018;
[26] *http://www.itmeteodata.com/itmeteotry-fotovoltaico.html*, accesed on april 2016.
[27] I. Sengor, H. C. Kilickiran, H. Akdemir, B. Kekezoglu, O. Erdinc; and J. P. S. Catalão, "Energy management of a smart railway station considering regenerative braking and stochastic behaviour of ESS and PV generation", *IEEE Trans. Sustainable Energy*, in press.

VII. BIOGRAPHIES

Salvatore D'Arco received the M.Sc. and Ph.D. degrees in electrical engineering from the University of Naples "Federico II," Naples, Italy, in 2002 and 2005, respectively.
From 2006 to 2007, he was a postdoctoral researcher at the University of South Carolina, Columbia, SC, USA. In 2008, he joined ASML, Veldhoven, the Netherlands, as a Power Electronics Designer, where he worked until 2010. From 2010 to 2012, he was a postdoctoral researcher in the Department of Electric Power Engineering at the Norwegian University of Science and Technology (NTNU), Trondheim, Norway. In 2012, he joined SINTEF Energy Research where he currently works as a Research Scientist. He is the author of more than 90 scientific papers and is the holder of one patent. His main research activities are related to control and analysis of power-electronic conversion systems for power system applications, including real-time simulation and rapid prototyping of converter control systems.

Luigi Piegari (M'04–SM'13) was born in Naples, Italy, on April 2, 1975. He received the M.S. (cum laude) and Ph.D. degrees in electrical engineering from the University of Naples Federico II, Naples, Italy, in 1999 and 2003, respectively.
From 2003 to 2008, he was a Postdoctoral Research Fellow with the Department of Electrical Engineering, University of Naples Federico II. From 2009 to 2012, he was an Assistant Professor with the Department of Electrical Engineering, Polytechnic University of Milan, Milan, Italy. He is currently an Associate Professor of power electronics, electrical machines and drives with the Department of Electronics, Information and Bioengineering, Politecnico di Milano. He has authored or co-authored more than 150 scientific papers published in international journals and conference proceedings. His research interests include storage devices modelling and ageing, wind and photovoltaic generation, modelling and control of multilevel converters, electrical drives, and dc protection and distribution grids.
Prof. Piegari is a member of the IEEE Industrial Electronics Society, the IEEE Power Electronics Society, and AEIT. He is the Technical Program Chair of the International Conference on Clean Electrical Power.

Pietro Tricoli (M'06) was born in Naples, Italy, on September 8, 1978. He received the MSc (*cum laude*) and PhD degrees in electrical engineering from the University of Naples Federico II, Italy, in 2002 and 2005, respectively.
He was a Visiting Scholar in the Department of Electrical and Computer Engineering, University of Wisconsin-Madison, Madison, in 2005. In 2006, he was also a Visiting Scholar in the Department of Electrical and Electronic Engineering, Nagasaki University, Nagasaki, Japan. From 2006 to 2011, he was a Postdoctoral Research Fellow with the Department of Electrical Engineering, University of Naples Federico II, Italy. He is currently a Senior Lecturer in Electrical Power and Control in the Department of Electronic, Electrical, and Systems Engineering, University of Birmingham, Birmingham, U.K. He is the author of more than 80 scientific papers published in international journals and conference proceedings. His research interests include the modelling of storage devices for road electric vehicles, railways, and rapid transit systems, wind and photovoltaic generation, and the modelling and control of multilevel converters.
Dr Tricoli is a member of the IEEE Industrial Electronics Society and the Energy Institute. He is an associate editor of the IET journal Renewable Power Generation and the Web & Publication Chair of the International Conference on Clean Electrical Power. He is a Registered Professional Engineer in Italy.